Chinese Journal of Aeronautics, 2013,26(4): 909–917

Chinese Society of Aeronautics and Astronautics
& Beihang University

Chinese Journal of Aeronautics

cja@buaa.edu.cn
www.sciencedirect.com

Gain self-scheduled H_∞ control for morphing aircraft in the wing transition process based on an LPV model

Yue Ting [a,*], Wang Lixin [a], Ai Junqiang [b]

[a] *School of Aeronautic Science and Engineering, Beihang University, Beijing 100191, China*
[b] *The First Aircraft Design Institute of AVIC, Xi'an 710089, China*

Received 21 May 2012; revised 7 September 2012; accepted 10 January 2013
Available online 2 July 2013

KEYWORDS

Gain self-scheduled;
H_∞ robust control;
Linear parameter varying;
Morphing aircraft;
Wing transition

Abstract This article investigates gain self-scheduled H_∞ robust control system design for a tailless folding-wing morphing aircraft in the wing shape varying process. During the wing morphing phase, the aircraft's dynamic response will be governed by time-varying aerodynamic forces and moments. Nonlinear dynamic equations of the morphing aircraft are linearized by using Jacobian linearization approach, and a linear parameter varying (LPV) model of the morphing aircraft in wing folding is obtained. A multi-loop controller for the morphing aircraft is formulated to guarantee stability for the wing shape transition process. The proposed controller uses a set of inner-loop gains to provide stability using classical techniques, whereas a gain self-scheduled H_∞ outer-loop controller is devised to guarantee a specific level of robust stability and performance for the time-varying dynamics. The closed-loop simulations show that speed and altitude vary slightly during the whole wing folding process, and they converge rapidly after the process ends. This proves that the gain self-scheduled H_∞ robust controller can guarantee a satisfactory dynamic performance for the morphing aircraft during the whole wing shape transition process. Finally, the flight control system's robustness for the wing folding process is verified according to uncertainties of the aerodynamic parameters in the nonlinear model.

1. Introduction

Morphing aircraft can automatically change its aerodynamic configuration to adapt to different flight environments and combat missions by using advanced materials and actuators.[1,2] Compared to conventional fixed-wing aircraft, morphing aircraft possesses multi-objective adaptability and higher combat effectiveness.[3,4] The typical objective of morphing aircraft design includes enhancing flight performance and combat effectiveness, but not improving the flying quality. So application of morphing techniques may bring disadvantage to the aircraft's dynamic characteristics.

The wing transition process is obviously complicated and very important for morphing aircraft. Generally, the wing morphing approach will involve large rigid-body motions of the wing structure. The dynamic response of morphing aircraft will be governed by time-varying aerodynamic forces and moments which are related to the wing shape. Dynamic models for morphing aircraft must take into account the dynamic

* Corresponding author. Tel.: +86 10 82338821.
E-mail addresses: yueting_buaa@sina.com (T. Yue), bhu_wlx@tom.com (L. Wang).

Peer review under responsibility of Editorial Committee of CJA.

ELSEVIER Production and hosting by Elsevier

1000-9361 © 2013 Production and hosting by Elsevier Ltd. on behalf of CSAA & BUAA. Open access under CC BY-NC-ND license.
http://dx.doi.org/10.1016/j.cja.2013.06.004

coupling between wing area and mass distribution change, aerodynamics, structure, and control forces. Thus, the wing morphing process is a complicated time-varying dynamic system.[5–7] As wing configuration parameters and aerodynamics do vary in large ranges, the dynamic response in wing morphing and the final balanced kinetic parameters will also exhibit large variations. Furthermore, the aircraft needs a long time to achieve a new state of level flight without control. Consequently, the flying quality of morphing aircraft may deteriorate and flight safety may be threatened. To guarantee satisfactory flying quality, a morphing aircraft capable of shape reconfiguration requires a flight control system to maintain stability during the morphing transition phase.

Current research on flight control design for morphing aircraft mainly focuses on static configuration control.[8–11] There is a notable lack of published work on flight control design for morphing aircraft's wing transition phase. When the aerodynamic shape is changing, the controller should adapt online to maintain stability in shape transition between different configurations. Since the wing transition process is time-varying, it is obviously quite difficult to use general control techniques to control such a complex dynamic behavior. One possible approach is to assume that the time-varying dynamics could be represented by a linear parameter varying (LPV) plant model that approximately captures the wing transition phase's complex behavior. In this LPV framework, nonlinear dynamic equations of morphing aircraft could be simplified and transformed to an LPV model. Then gain self-scheduled control technique[12–14] based on the LPV model could be used for wing transition control. The gain self-scheduled control technique based on the LPV model can rapidly change controller parameters to adapt to the aircraft's dynamic response. Additionally, this control approach can guarantee stability of the closed-loop system. Therefore, the gain self-scheduled control technique can be utilized to solve flight control design problems for the wing transition process of morphing aircraft.

This article focuses on gain self-scheduled H_∞ robust control design during the wing folding process of a tailless folding-wing morphing aircraft. According to the properties of wing folding process, longitudinal nonlinear dynamic equations of the morphing aircraft in wing shape varying are simplified and transformed to an LPV model. Then, a multi-loop controller designed based on the LPV model is presented. It is found that this control approach can successfully maintain stability for the morphing aircraft in the whole wing transition process.

2. Gain self-scheduled H_∞ robust control for LPV system

The class of finite dimensional linear systems whose state-space matrixes depend continuously on a time varying parameter vector $\boldsymbol{\theta}(t)$ is called linear parameter varying. In state-space form, an LPV system model can be expressed as

$$\begin{cases} \dot{\boldsymbol{x}} = \boldsymbol{A}(\boldsymbol{\theta}(t))\boldsymbol{x} + \boldsymbol{B}(\boldsymbol{\theta}(t))\boldsymbol{u} \\ \boldsymbol{y} = \boldsymbol{C}(\boldsymbol{\theta}(t))\boldsymbol{x} + \boldsymbol{D}(\boldsymbol{\theta}(t))\boldsymbol{u} \end{cases} \tag{1}$$

where the state matrixes $\boldsymbol{A}$, $\boldsymbol{B}$, $\boldsymbol{C}$, $\boldsymbol{D}$ vary with $\boldsymbol{\theta}(t)$, $\boldsymbol{u}$ is the control input. It is a time-varying vector that can consist of system outputs, exogenous inputs, or combinations of both. LPV systems are linear systems where the state-space description is an explicit function of $\boldsymbol{\theta}(t)$.

Here we focus on the standard H_∞ control problem of LPV system. As shown in Fig. 1, the resulting LPV controller $\boldsymbol{K}(\theta)$ exploits all available information on $\boldsymbol{\theta}(t)$ to adjust the current plant's dynamics. This provides smooth and automatic gain self-scheduled with respect to the varying parameter $\boldsymbol{\theta}(t)$.

We consider LPV plants $\boldsymbol{P}(\boldsymbol{\theta})$ with state-space equations

$$\begin{cases} \dot{\boldsymbol{x}} = \boldsymbol{A}(\boldsymbol{\theta})\boldsymbol{x} + \boldsymbol{B}_1(\boldsymbol{\theta})\boldsymbol{w} + \boldsymbol{B}_2(\boldsymbol{\theta})\boldsymbol{u} \\ \boldsymbol{z} = \boldsymbol{C}_1(\boldsymbol{\theta})\boldsymbol{x} + \boldsymbol{D}_{11}(\boldsymbol{\theta})\boldsymbol{w} + \boldsymbol{D}_{12}(\boldsymbol{\theta})\boldsymbol{u} \\ \boldsymbol{y} = \boldsymbol{C}_2(\boldsymbol{\theta})\boldsymbol{x} + \boldsymbol{D}_{21}(\boldsymbol{\theta})\boldsymbol{w} + \boldsymbol{D}_{22}(\boldsymbol{\theta})\boldsymbol{u} \end{cases} \tag{2}$$

with state $\boldsymbol{x} \in \mathbf{R}^n$, disturbance $\boldsymbol{w} \in \mathbf{R}^{m_1}$, control input $\boldsymbol{u} \in \mathbf{R}^{m_2}$, performance output $\boldsymbol{z} \in \mathbf{R}^{p_1}$, and measured output $\boldsymbol{y} \in \mathbf{R}^{p_2}$.

The plants $\boldsymbol{P}(\boldsymbol{\theta})$ can be described as

$$\boldsymbol{P} = \begin{bmatrix} \boldsymbol{P}_{11} & \boldsymbol{P}_{12} \\ \boldsymbol{P}_{21} & \boldsymbol{P}_{22} \end{bmatrix} = \begin{bmatrix} \boldsymbol{A}(\boldsymbol{\theta}) & \boldsymbol{B}_1(\boldsymbol{\theta}) & \boldsymbol{B}_2(\boldsymbol{\theta}) \\ \boldsymbol{C}_1(\boldsymbol{\theta}) & \boldsymbol{D}_{11}(\boldsymbol{\theta}) & \boldsymbol{D}_{12}(\boldsymbol{\theta}) \\ \boldsymbol{C}_2(\boldsymbol{\theta}) & \boldsymbol{D}_{21}(\boldsymbol{\theta}) & \boldsymbol{D}_{22}(\boldsymbol{\theta}) \end{bmatrix} \tag{3}$$

We seek an LPV controller $\boldsymbol{K}(\boldsymbol{\theta})$ of the form

$$\begin{cases} \dot{\boldsymbol{x}}_K = \boldsymbol{A}_K(\boldsymbol{\theta})\boldsymbol{x}_K + \boldsymbol{B}_K(\boldsymbol{\theta})\boldsymbol{y} \\ \boldsymbol{u} = \boldsymbol{C}_K(\boldsymbol{\theta})\boldsymbol{x}_K + \boldsymbol{D}_K(\boldsymbol{\theta})\boldsymbol{y} \end{cases} \tag{4}$$

that guarantees H_∞ performance for the closed-loop system in Fig. 1. The transfer function from w to z of the closed-loop system is

$$\boldsymbol{T}_{zw}(s) = \boldsymbol{P}_{11} + \boldsymbol{P}_{12}\boldsymbol{K}(\boldsymbol{I} - \boldsymbol{P}_{22}\boldsymbol{K})^{-1}\boldsymbol{P}_{21} \tag{5}$$

Definition 1. [15]A matrix polytope is defined as convex hull of a finite number of matrices $\boldsymbol{N}_i$ with the same dimensions, i.e.,

$$\mathrm{Co}\{\boldsymbol{N}_i, i = 1, 2, \cdots, r\} := \left\{ \sum_{i=1}^{r} \alpha_i \boldsymbol{N}_i : \alpha_i \geqslant 0, \sum_{i=1}^{r} \alpha_i = 1 \right\} \tag{6}$$

where α_i is the weighting ratio. For the LPV system Eq. (2), if: (A) the parameter dependence is affine, that is, the state-space matrices $\boldsymbol{A}(\boldsymbol{\theta})$, $\boldsymbol{B}_1(\boldsymbol{\theta})$, $\boldsymbol{B}_2(\boldsymbol{\theta})$, $\boldsymbol{C}_1(\boldsymbol{\theta})$, $\boldsymbol{C}_2(\boldsymbol{\theta})$, $\boldsymbol{D}_{11}(\boldsymbol{\theta})$, $\boldsymbol{D}_{12}(\boldsymbol{\theta})$, $\boldsymbol{D}_{21}(\boldsymbol{\theta})$ and $\boldsymbol{D}_{22}(\boldsymbol{\theta})$ depend affinely on $\boldsymbol{\theta}$; (B) the tine-varying parameter $\boldsymbol{\theta}$ varies in a polytope $\boldsymbol{\Theta}$, that is $\boldsymbol{\theta} \in \boldsymbol{\Theta} = Co\{\boldsymbol{\theta}_1, \boldsymbol{\theta}_2, \ldots, \boldsymbol{\theta}_r\}$; the plant is further assumed to be polytopic, i.e.,

$$\begin{bmatrix} \boldsymbol{A}(\boldsymbol{\theta}) & \boldsymbol{B}_1(\boldsymbol{\theta}) & \boldsymbol{B}_2(\boldsymbol{\theta}) \\ \boldsymbol{C}_1(\boldsymbol{\theta}) & \boldsymbol{D}_{11}(\boldsymbol{\theta}) & \boldsymbol{D}_{12}(\boldsymbol{\theta}) \\ \boldsymbol{C}_2(\boldsymbol{\theta}) & \boldsymbol{D}_{21}(\boldsymbol{\theta}) & \boldsymbol{D}_{22}(\boldsymbol{\theta}) \end{bmatrix} \in \mathrm{Co}\left\{ \begin{bmatrix} \boldsymbol{A}_i & \boldsymbol{B}_{1i} & \boldsymbol{B}_{2i} \\ \boldsymbol{C}_{1i} & \boldsymbol{D}_{11i} & \boldsymbol{D}_{12i} \\ \boldsymbol{C}_{2i} & \boldsymbol{D}_{21i} & \boldsymbol{D}_{22i} \end{bmatrix}, i = 1, 2, \cdots, r \right\} \tag{7}$$

where $\boldsymbol{A}_i$, $\boldsymbol{B}_{1i}$, …, denote the values of $\boldsymbol{A}(\boldsymbol{\theta})$, $\boldsymbol{B}_1(\boldsymbol{\theta})$, …, at the vertices $\boldsymbol{\theta} = \boldsymbol{\theta}_i$ of the parameter polytope.

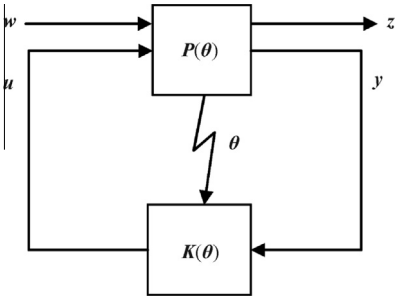

Fig. 1 LPV control of LPV system.

In the sequel the standard H_∞ control problem can be defined as: finding an internally stabilizing controller $\boldsymbol{K}$ that makes the closed-loop H_∞ gain from $\boldsymbol{w}$ to $\boldsymbol{z}$ less than γ. If $\boldsymbol{T}_{zw}(s)$ denotes the closed-loop transfer function $\boldsymbol{w}$ to $\boldsymbol{z}$, this control objective can be formalized as

$$\|\boldsymbol{T}_{zw}(s)\|_\infty < \gamma \tag{8}$$

It is known from Ref. [15] that there exists an LPV controller Eq. (4) guaranteeing quadratic H_∞ performance γ along all parameter trajectories, if and only if there exist two symmetric matrices $\mathbf{R} \in \mathbf{R}^{n\times n}$ and $\mathbf{S} \in \mathbf{R}^{n\times n}$ satisfying the system of $2r + 1$ linear matrix inequalities (LMI).

If $\boldsymbol{\theta}$ is in the polytope $\mathrm{Co}\{\boldsymbol{\theta}_1, \boldsymbol{\theta}_2, \ldots, \boldsymbol{\theta}_r\}$, that is,

$$\boldsymbol{\theta} \in \boldsymbol{\Theta} := \left\{ \sum_{i=1}^{r} \alpha_i \boldsymbol{\theta}_i : \alpha_i \geqslant 0, \sum_{i=1}^{r} \alpha_i = 1 \right\} \tag{9}$$

Then the LPV controller's state-space matrices are given by

$$\begin{bmatrix} \boldsymbol{A}_K(\boldsymbol{\theta}(t)) & \boldsymbol{B}_K(\boldsymbol{\theta}(t)) \\ \boldsymbol{C}_K(\boldsymbol{\theta}(t)) & \boldsymbol{D}_K(\boldsymbol{\theta}(t)) \end{bmatrix} := \sum_{i=1}^{r} \alpha_i(t) \begin{bmatrix} \boldsymbol{A}_{Ki} & \boldsymbol{B}_{Ki} \\ \boldsymbol{C}_{Ki} & \boldsymbol{D}_{Ki} \end{bmatrix} \tag{10}$$

where $\boldsymbol{A}_{Ki}$, $\boldsymbol{B}_{Ki}$, $\boldsymbol{C}_{Ki}$, $\boldsymbol{D}_{Ki}$ can be obtained off-line, and $\boldsymbol{A}_K(\boldsymbol{\theta}(t))$, $\boldsymbol{B}_K(\boldsymbol{\theta}(t))$, $\boldsymbol{C}_K(\boldsymbol{\theta}(t))$, $\boldsymbol{D}_K(\boldsymbol{\theta}(t))$ will update dependently on the parameter $\boldsymbol{\theta}(t)$ in real time.

3. Longitudinal LPV model in wing shape varying for folding-wing morphing aircraft

In this article a folding-wing morphing aircraft which has a tailless flying wing configuration is studied (shown in Fig. 2). The wings include inner wings and outer wings, which can be folded by smart actuators to change their shape. In the wing transition process, the inner wings rotate and the outer wings keep level.

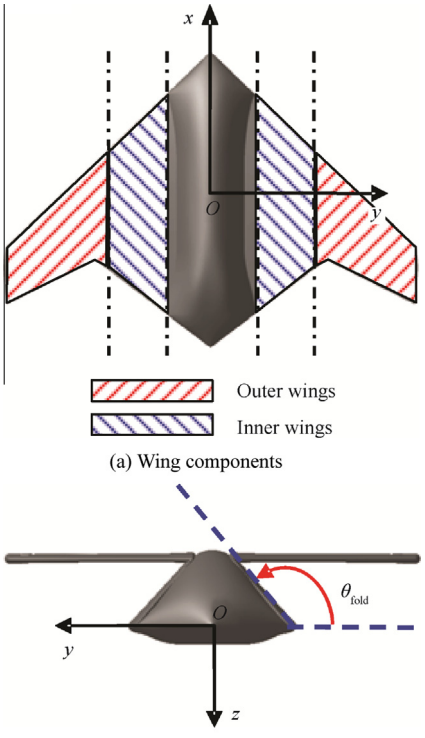

Fig. 2 Folding-wing morphing aircraft.

When the wing shape is changing, the dynamic response of the morphing aircraft will be dependent on time-varying aerodynamic forces and moments, which are both functions of the wing shape. In Ref. [16] the folding-wing morphing aircraft is regarded as a variable geometry rigid body, and a six-DOF nonlinear dynamic model in the wing folding process is founded. It also shows that the aerodynamic forces and moments of the folding-wing morphing aircraft almost linearly vary with the wing fold angle θ_{fold} in wing folding. Hence, we can regard the morphing process as an LPV system. In this LPV framework, the nonlinear dynamic equations of the morphing aircraft will be simplified and transformed to an LPV model by LPV modeling approaches.[17–20]

Here we only consider the longitudinal motion of the aircraft during the wing folding process. The longitudinal nonlinear equations of motion in the wing folding process can be expressed as[16]

$$\begin{cases} \dot{V}_x = \dfrac{I_y}{mI_y - S_z^2}(-mqV_z - 2q\dot{S}_z + F_x) \\ \qquad - \dfrac{S_z}{mI_y - S_z^2}\left(-\dot{I}_y q - S_z q V_z + \dfrac{2S_{1x}\ddot{S}_{1z}}{m_1} + \dfrac{2S_{2x}\ddot{S}_{2z}}{m_2} + M_y\right) \\ \dot{V}_z = \dfrac{1}{m}(mqV_x + q^2 S_z - \ddot{S}_z + F_z) \\ \dot{q} = -\dfrac{S_z}{mI_y - S_z^2}(-mqV_z - 2q\dot{S}_z + F_x) \\ \qquad + \dfrac{m}{mI_y - S_z^2}\left(-\dot{I}_y q - S_z q V_z + \dfrac{2S_{1x}\ddot{S}_{1z}}{m_1} + \dfrac{2S_{2x}\ddot{S}_{2z}}{m_2} + M_y\right) \\ \dot{\theta} = q \end{cases} \tag{11}$$

The variables in Eq. (11) are introduced in Ref.[16] It is assumed that the thrust line passes through the origin of the fixed-body axes. The forces and moments in right-hand side of Eq. (11) can be expressed as

$$\begin{cases} F_x = -D\cos\alpha + L\sin\alpha + T - mg\sin\theta \\ F_z = -D\sin\alpha - L\cos\alpha + mg\cos\theta \\ M_y = M_{\text{A}} - gS_z\sin\theta \end{cases} \tag{12}$$

where D, L, T are the drag, lift and thrust, M_{A} is the pitching moment caused by aerodynamic forces, α the angle of attack, θ the pitch angle, S_z the z-component of static momentum $S = \int r \times \mathrm{d}m$ in fixed-body axes, and g the acceleration due to gravity, respectively. The lift, drag, and pitching moments in Eq. (12) are given as

$$\begin{cases} L = \dfrac{1}{2}\rho V^2 S C_L \\ D = \dfrac{1}{2}\rho V^2 S C_D \\ M_A = \dfrac{1}{2}\rho V^2 S c C_m \end{cases} \tag{13}$$

where ρ is the air density, S the wing area, and c the mean aerodynamic chord. The lift, drag and pitching moment coefficients are given as

$$\begin{cases} C_L = C_L(\alpha, V) = C_{L0} + C_{L\alpha}\alpha + C_{LV}\Delta V/V + C_{L\delta_e}\delta_e \\ C_D = C_D(\alpha, V) = C_{D0} + C_{D\alpha}\alpha + C_{D\alpha^2}\alpha^2 + C_{DV}\Delta V/V + C_{D\delta_e}\delta_e \\ C_m = C_m(\alpha, q, V, \delta_e) = C_{m0} + C_{m\alpha}\alpha + C_{mV}\Delta V/V + C_{mq}q + C_{m\delta_e}\delta_e \end{cases} \tag{14}$$

The variables in Eq. (14) are given in Ref.[16] By combining Eqs. (11)–(14) and using Jacobian linearization approach, we get the LPV model presented in state-space form as

$$\begin{bmatrix} \dot{u} \\ \dot{w} \\ \dot{q} \\ \dot{\theta} \end{bmatrix} = \boldsymbol{A}(\boldsymbol{\theta}(t)) \begin{bmatrix} u - u_0 \\ w - w_0 \\ q \\ \theta - \theta_0 \end{bmatrix} + \boldsymbol{B}(\boldsymbol{\theta}(t)) \begin{bmatrix} \Delta\delta_e \\ \Delta\delta_T \end{bmatrix} + \boldsymbol{W}(\boldsymbol{\theta}(t)) \quad (15)$$

where u, w are the x and z components of airspeed in fixed-body axes, u_0, w_0 the x and z components of balanced airspeed in fixed-body axes before wing folding, $V = \sqrt{u^2 + w^2}$, $\Delta\delta_T$ is the propulsion control, and θ_0 the initial pitch angle. $\boldsymbol{W}(\boldsymbol{\theta}(t))$ is the force and moment variations affected by wing folding, which can be considered as a disturbance source in the wing morphing dynamic response. In Eq. (15) the state-space matrices vary with θ_{fold}, and terms in the matrices are given in Appendix A.

When using Jacobian linearization approach to transform nonlinear model to an LPV model, the dynamic response of morphing transition phase produced by the two models should be similar, i.e., the obtained LPV model should be rational. Parameter comparisons of the dynamic response of the two different models are shown in Fig. 3, in which it can be seen that distinctions between the dynamic responses in LPV model and nonlinear model are small. The LPV model is able to capture the dynamic behavior and match the nonlinear model. Therefore, the control system design of the morphing aircraft in wing folding can be based on the LPV model. Keeping the altitude and speed constant during wing shape varying can 'be the control objective. According to the property of the LPV model, LPV control techniques could be chosen to guarantee smooth transition between different configurations.

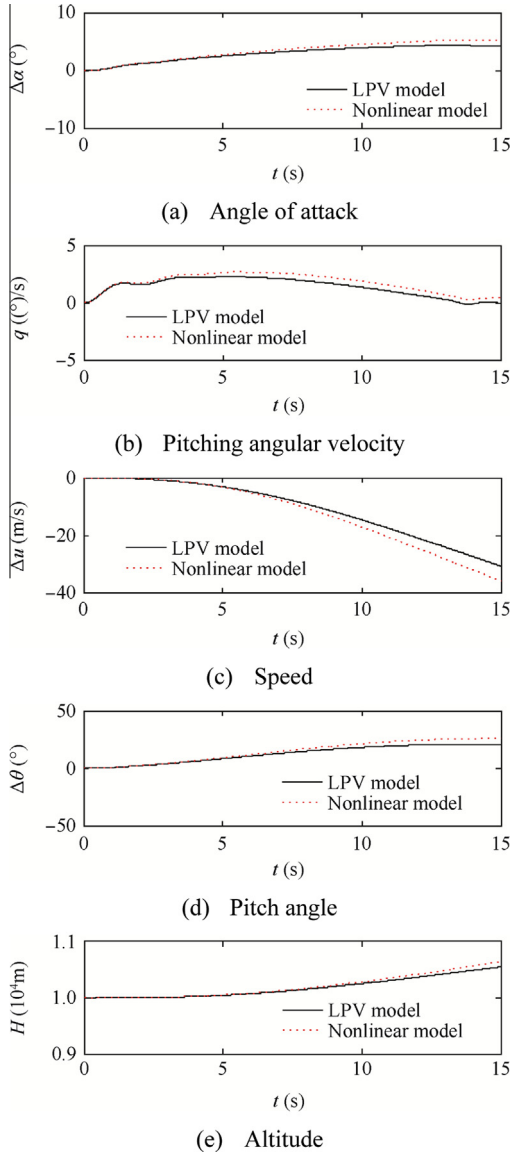

Fig. 3 LPV vs nonlinear model simulations of morphing aircraft.

The initial dynamic response of the wing folding process mainly represents variations in the aircraft's pitching moment. The aerodynamic forces acting on the aircraft change a little. Then the speed and altitude vary only slightly, and α, θ, q all increase as the pitching moment in zero lift increases when the wing begins to fold. When the wing continues to fold, α and q gradually converge, the altitude increases and the speed decreases, indicating that the aircraft begins to climb with decreasing speed. Every parameter will converge to a stable value after a long period of time and the aircraft will enter a new state of balanced flight.

In the wing folding process of the tailless folding-wing aircraft, the altitude, speed and pitch angle vary largely, and the aircraft will need a long time to achieve new stable flight. In order to guarantee satisfactory flying quality and safety in the process of wing folding, a flight control system is required.

4. Multi-loop controller design and simulation for the wing morphing process

We know from the dynamic response of the folding-wing morphing aircraft in transition phase that the altitude and speed do change a lot. Moreover, it takes a long time for the aircraft to achieve new balance in stable flight. To ensure that the morphing aircraft can maintain stable flight during wing shape varying, the wing morphing process needs a flight control system to obtain a prospective objective. In this article, the control objective is to keep the altitude and speed constant during the transition from extended-wing configuration to folded-wing configuration.

The longitudinal LPV model of the morphing aircraft in morphing can be rewritten as

$$\dot{\boldsymbol{x}} = \boldsymbol{A}(\boldsymbol{\theta}(t))\boldsymbol{x} + \boldsymbol{B}(\boldsymbol{\theta}(t))\boldsymbol{u} + \boldsymbol{B}_1\boldsymbol{w}(\boldsymbol{\theta}(t)) \quad (16)$$

where $\boldsymbol{x} \in \mathbf{R}^4$, $\boldsymbol{u} \in \mathbf{R}^2$, $\boldsymbol{w} \in \mathbf{R}^{4\times1}$, $\boldsymbol{A} \in \mathbf{R}^{4\times4}$, $\boldsymbol{B} \in \mathbf{R}^{4\times2}$, $\boldsymbol{B}_1 = \boldsymbol{I}^4$.

Considering $\boldsymbol{w}(\boldsymbol{\theta}(t))$ as a disturbance, then the system can be regarded as an LPV system $\dot{\boldsymbol{x}} = \boldsymbol{A}(\boldsymbol{\theta}(t))\boldsymbol{x} + \boldsymbol{B}(\boldsymbol{\theta}(t))\boldsymbol{u}$ with a disturbance $\boldsymbol{w}(\boldsymbol{\theta}(t))$. Therefore, the flight control objective is to keep the altitude and speed stable when the system $\dot{\boldsymbol{x}} = \boldsymbol{A}(\boldsymbol{\theta}(t))\boldsymbol{x} + \boldsymbol{B}(\boldsymbol{\theta}(t))\boldsymbol{u}$ is disturbed by $\boldsymbol{w}(\boldsymbol{\theta}(t))$.

According to the property of the LPV system, the inner loop of the control system is a linear quadratic output feedback controller which provides stability, as well as tracking performance characteristics for the linear system $\dot{\boldsymbol{x}} = \boldsymbol{A}(\boldsymbol{\theta}(t))\boldsymbol{x} + \boldsymbol{B}(\boldsymbol{\theta}(t))\boldsymbol{u}$. The outer loop is composed of a gain self-scheduled robust H_∞ controller which can be solved by using a convex hull algorithm. The multi-loop controller is shown in Fig. 4.

4.1. Inner-loop linear quadratic optimal control with output feedback

The controller design objective in wing transition phase for the folding-wing morphing aircraft is to keep the altitude and

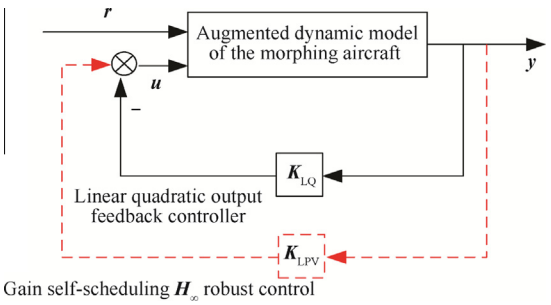

Fig. 4 The multi-loop control structure.

speed constant. The inner-loop of the control system is an LQ optimal controller with output feedback, as shown in Fig. 5.

The augmented state equations of the system shown in Fig. 5 can be expressed in the form of

$$\begin{cases} \dot{\boldsymbol{x}} = \boldsymbol{A}\boldsymbol{x} + \boldsymbol{B}\boldsymbol{u} + \boldsymbol{G}\boldsymbol{r} \\ \boldsymbol{y} = \boldsymbol{C}\boldsymbol{x} + \boldsymbol{F}\boldsymbol{r} \\ \boldsymbol{z} = \boldsymbol{H}\boldsymbol{x} \end{cases} \tag{17}$$

where

$$\begin{cases} \boldsymbol{x} = [\Delta u \quad \Delta w \quad \Delta q \quad \Delta\theta \quad \Delta H \quad \delta_e \quad \delta_T \quad \varepsilon_H \quad \varepsilon_u]^T \\ \boldsymbol{y} = [\Delta q \quad \Delta\theta \quad e_H \quad \varepsilon_H \quad e_u \quad \varepsilon_u]^T \\ \boldsymbol{z} = [\Delta H \quad \Delta u]^T \\ \boldsymbol{u} = [\delta_e \quad \delta_T]^T \end{cases} \tag{18}$$

With this structure, the plant matrices are given by

$$A = \begin{bmatrix} a_{11} & a_{12} & a_{13} & a_{14} & 0 & b_{11} & b_{12} & 0 & 0 \\ a_{21} & a_{22} & a_{23} & a_{24} & 0 & b_{21} & b_{22} & 0 & 0 \\ a_{31} & a_{32} & a_{33} & a_{34} & 0 & b_{31} & b_{32} & 0 & 0 \\ a_{41} & a_{42} & a_{43} & a_{44} & 0 & b_{41} & b_{42} & 0 & 0 \\ 0 & -1 & 0 & u_0 & 0 & 0 & 0 & 0 & 0 \\ 0 & 0 & 0 & 0 & 0 & -20 & 0 & 0 & 0 \\ 0 & 0 & 0 & 0 & 0 & 0 & -2 & 0 & 0 \\ 0 & 0 & 0 & 0 & -1 & 0 & 0 & 0 & 0 \\ -1 & 0 & 0 & 0 & 0 & 0 & 0 & 0 & 0 \end{bmatrix} \tag{19}$$

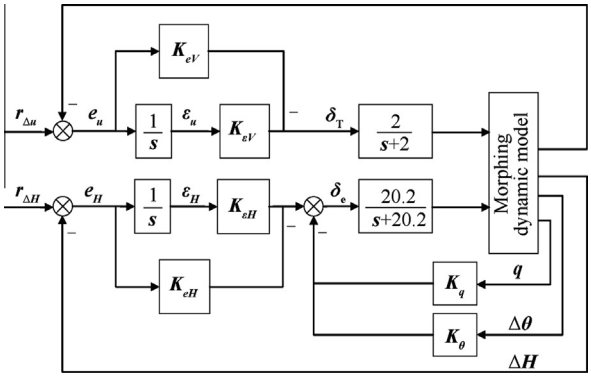

Fig. 5 Inner-loop output feedback control structure.

$$B = \begin{bmatrix} 0 & 0 \\ 0 & 0 \\ 0 & 0 \\ 0 & 0 \\ 0 & 0 \\ 20 & 0 \\ 0 & 2 \\ 0 & 0 \\ 0 & 0 \end{bmatrix} \tag{20}$$

$$C = \begin{bmatrix} 0 & 0 & 1 & 0 & 0 & 0 & 0 & 0 & 0 \\ 0 & 0 & 0 & 1 & 0 & 0 & 0 & 0 & 0 \\ 0 & 0 & 0 & 0 & -1 & 0 & 0 & 0 & 0 \\ 0 & 0 & 0 & 0 & 0 & 0 & 0 & 1 & 0 \\ -1 & 0 & 0 & 0 & 0 & 0 & 0 & 0 & 0 \\ 0 & 0 & 0 & 0 & 0 & 0 & 0 & 0 & 1 \end{bmatrix} \tag{21}$$

$$H = \begin{bmatrix} 0 & 0 & 0 & 0 & 1 & 0 & 0 & 0 & 0 \\ 1 & 0 & 0 & 0 & 0 & 0 & 0 & 0 & 0 \end{bmatrix} \tag{22}$$

$$F = \begin{bmatrix} 0 & 0 & 1 & 0 & 0 & 0 \\ 0 & 0 & 0 & 0 & 1 & 0 \end{bmatrix}^T \tag{23}$$

$$G = \begin{bmatrix} 0 & 0 & 0 & 0 & 0 & 0 & 0 & 1 & 0 \\ 0 & 0 & 0 & 0 & 0 & 0 & 0 & 0 & 0 \end{bmatrix}^T \tag{24}$$

According to Fig. 5, the control input is given by

$$u = -K_{LQ}y = -\begin{bmatrix} K_q & K_\theta & K_{eH} & K_{\varepsilon H} & 0 & 0 \\ 0 & 0 & 0 & 0 & K_{eu} & K_{\varepsilon u} \end{bmatrix} y \tag{25}$$

In the augmented description, the gains K_q, K_θ, K_{eH}, $K_{\varepsilon H}$, K_{eu} and $K_{\varepsilon u}$ are unknown, and need to be selected to yield acceptable closed-loop performance.

To solve the output gain problem, Stevens and Lewis[21] devised the conversion from tracking to a regulator problem, using a new set of deviation variables. To make both the error deviation $\tilde{e}(t)$ and the steady-state error $\bar{e}$ small, the output gain $\boldsymbol{K}$ is selected to minimize the performance index (PI)

$$J = \frac{1}{2}\int_0^\infty (\tilde{e}^T\tilde{e} + \tilde{u}^T R\tilde{u})\mathrm{d}t + \frac{1}{2}\bar{e}^T V\bar{e} \tag{26}$$

with $\boldsymbol{R} > 0$, $\boldsymbol{V} \geqslant 0$. The optimization problem can be solved numerically using an iterative procedure through Lyapunov equations.[22,23]

As the state-space matrices of the LPV model change with the wing fold angle θ_{fold}, the optimal output gain K_{LQ} will also change with corresponding θ_{fold}. Nevertheless, a time-invariant gain $\boldsymbol{K}_{LQ}$ is preferred, although only a suboptimal solution would be achieved in such a case. The performance of the closed-loop system in the wing folding process can be achieved by outer-loop self-scheduled H_∞ robust control design. Here we select the optimal output feedback gain in extended-wing configuration as the inner-loop gain:

$$K_{LQ} = \begin{bmatrix} -16.5 & -68.7 & 0.14 & 0.03 & 0 & 0 \\ 0 & 0 & 0 & 0 & -15.8 & -18.9 \end{bmatrix} \tag{27}$$

4.2. Outer-loop gain self-scheduled H_∞ robust control

The closed-loop system with LQ output feedback inner-loop controller is found to be

$$\begin{cases} \dot{\boldsymbol{x}} = \boldsymbol{A}_c(\boldsymbol{\theta}(t))\boldsymbol{x} + \boldsymbol{B}(\boldsymbol{\theta}(t))\boldsymbol{u} + \boldsymbol{B}_1\boldsymbol{w}(\boldsymbol{\theta}(t)) \\ \boldsymbol{z} = \boldsymbol{H}x \\ \boldsymbol{y} = \boldsymbol{C}x \end{cases} \tag{28}$$

where

$$\boldsymbol{A}_c(\boldsymbol{\theta}(t)) = \boldsymbol{A}(\boldsymbol{\theta}(t)) - \boldsymbol{B}(\boldsymbol{\theta}(t))\boldsymbol{K}_{\mathrm{LQ}}\boldsymbol{C}.$$

The gain self-scheduled H_∞ control problem consists in finding an LPV controller

$$\boldsymbol{u} = \boldsymbol{K}_{\mathrm{LPV}}(\boldsymbol{\theta})\boldsymbol{y} \tag{29}$$

to make the altitude and speed remain constant during the wing morphing process. The reference input $r = [\,r_{\Delta H} \quad r_{\Delta u}\,]^{\mathrm{T}} = \boldsymbol{0}$, and the outer-loop LPV control structure is shown in Fig. 6.

When using convex hull algorithm to design the LPV controller, if there are n variable elements in $\boldsymbol{A}_c(\boldsymbol{\theta}(t))$ and $\boldsymbol{B}(\boldsymbol{\theta}(t))$, the convex hull will have 2^n vertices. The calculation will be complicated if n is big. Therefore, we assume that the elements in $\boldsymbol{A}_c(\boldsymbol{\theta}(t))$ and $\boldsymbol{B}(\boldsymbol{\theta}(t))$ do not change as they vary in very small range. In other words, we only consider the elements that vary in large ranges during the wing folding process.

From the simplified LPV equations of morphing aircraft we find that the variable elements a_{22} and a_{32} in $\boldsymbol{A}_c(\boldsymbol{\theta}(t))$ vary in large ranges, which both depend on the aerodynamic changes during the wing folding process. Hereafter, the parameter vector of the LPV plant is denoted as $\boldsymbol{\theta}(t) := \begin{bmatrix} a_{22} \\ a_{32} \end{bmatrix}$. And

$$\begin{cases} a_{22} \subset [\,a_{22\min} \quad a_{22\max}\,] = [\,-1.3392 \quad -0.5212\,] \\ a_{32} \subset [\,a_{32\min} \quad a_{32\max}\,] = [\,-0.0618 \quad -0.0344\,] \end{cases} \tag{30}$$

So $\theta(t)$ ranges in the polytope $\boldsymbol{\Theta} \in \mathrm{Co}\{\boldsymbol{\theta}_i, i = 1, 2, 3, 4\}$. The vertices $\boldsymbol{\theta}_i$ are the values of $\boldsymbol{\theta}(t)$ at the four vertices of the parameter box: $\boldsymbol{\theta}_1 = \begin{bmatrix} a_{22\min} \\ a_{32\min} \end{bmatrix}$, $\boldsymbol{\theta}_2 = \begin{bmatrix} a_{22\max} \\ a_{32\min} \end{bmatrix}$, $\boldsymbol{\theta}_3 = \begin{bmatrix} a_{22\min} \\ a_{32\max} \end{bmatrix}$, $\boldsymbol{\theta}_4 = \begin{bmatrix} a_{22\max} \\ a_{32\max} \end{bmatrix}$.It is clear that the state-space matrix $\boldsymbol{A}_c(\boldsymbol{\theta}(t))$ ranges in a polytope of matrices whose vertices are the images of the vertices $\boldsymbol{\theta}_1$, $\boldsymbol{\theta}_2$, $\boldsymbol{\theta}_3$, $\boldsymbol{\theta}_4$. In other words,

$$\boldsymbol{A}_c(\boldsymbol{\theta}(t)) \in \mathrm{Co}\{A_i := A(\boldsymbol{\theta}_i), i = 1, 2, 3, 4\} \tag{31}$$

Finally, a formal expression for the LPV controller is derived by solving the convex decomposition problem. The following formulas for the state-space data of the LPV controller are obtained:

$$\begin{bmatrix} \boldsymbol{A}_K(\boldsymbol{\theta}(t)) & \boldsymbol{B}_K(\theta(t)) \\ \boldsymbol{C}_K(\boldsymbol{\theta}(t)) & \boldsymbol{D}_K(\boldsymbol{\theta}(t)) \end{bmatrix} := \sum_{i=1}^{4} \alpha_i(t) \begin{bmatrix} \boldsymbol{A}_{Ki} & \boldsymbol{B}_{Ki} \\ \boldsymbol{C}_{Ki} & \boldsymbol{D}_{Ki} \end{bmatrix} \tag{32}$$

It is easy to check that α_i are convex coordinates satisfying $\boldsymbol{\theta} \in \boldsymbol{\Theta} := \{\sum_{i=1}^{4} \alpha_i \boldsymbol{\theta}_i : \alpha_i \geqslant 0, \sum_{i=1}^{r} \alpha_i = 1\}$. The resulting polytopic LPV controller enforces stability and H_∞ performance over the entire parameter polytope $\boldsymbol{\Theta}$ and for arbitrary parameter variations.

4.3. Closed-loop simulation

The resulting gain self-scheduled H_∞ robust Controller based on the LPV model is applied at the morphing aircraft's wing

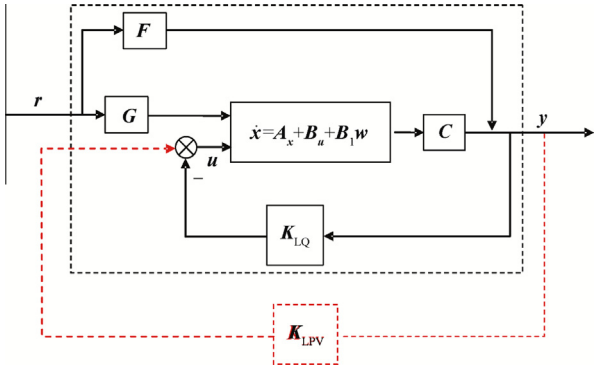

Fig. 6 Outer-loop LPV control structure.

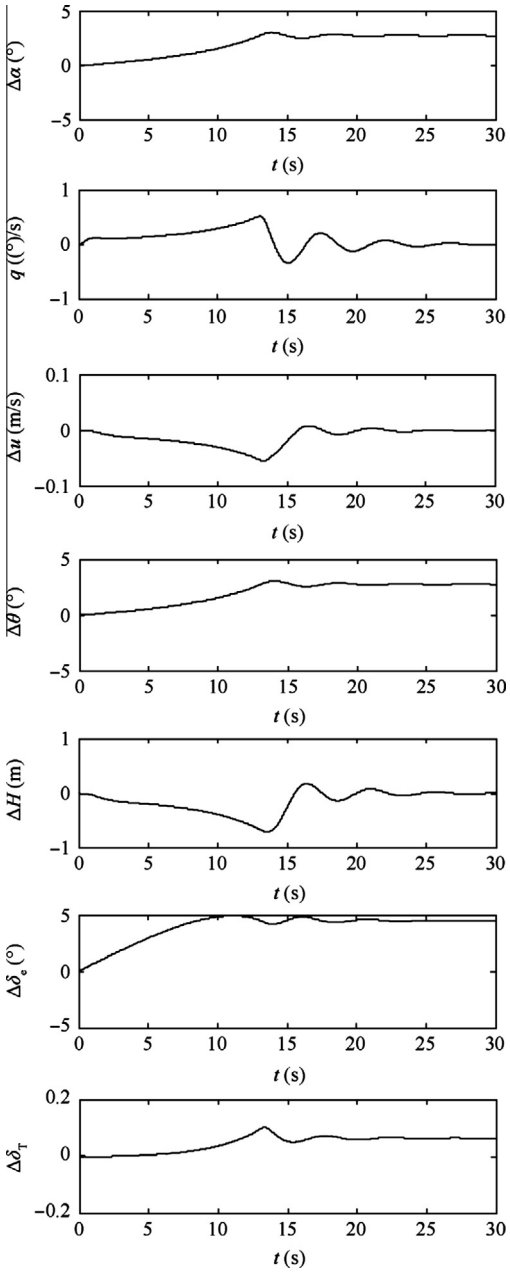

Fig. 7 Closed-loop response in morphing process.

shape transition phase. The response of the aircraft in closed-loop simulation is shown in Fig. 7. It is clear that the speed is almost constant and the altitude decreases about 0.7 m to the maximum during the wing folding process. They can both converge in 10 s after the wing finishes folding. Since the wing area decreases after it folds, the angle of attack will increase to achieve a new balance. In addition, the changes in elevator deflection and throttle are both within acceptable ranges. It is obvious that the gain self-scheduled H_∞ robust controller based on the morphing aircraft's LPV model can eliminate the disturbance caused by wing folding and guarantee constant-speed and altitude flight during the wing transition process.

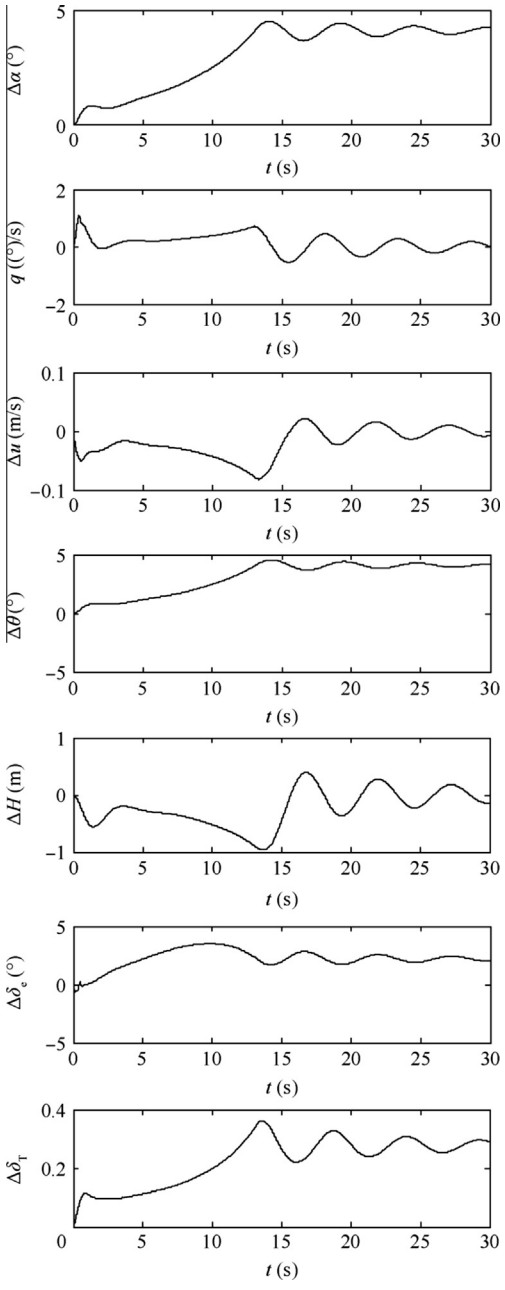

Fig. 8 Closed-loop response in parameter perturbation during wing folding process.

4.4. Robustness verification

In this article the aerodynamics in wing folding obtained by CFD is assumed to be quasi-steady, and unsteady aerodynamics is ignored. Consequently, the aerodynamics in the nonlinear model of the morphing aircraft is not modeled precisely, and not exactly the same with aerodynamics in actual flight conditions. In other words, the aerodynamic model of the wing folding process is uncertain within a range. Thus it is important for the controller to have the ability to provide stability in spite of modeling errors due to unmodeled dynamics and plant parameter variations.

The unpredictable manner of the model can be described by parameter perturbation. Here we use the parameter perturbation of the aerodynamic force and moment coefficients to describe model parameter perturbation. The aerodynamic coefficient perturbation is dependent on the angle of attack. When the angle of attack is bigger, the perturbation will be greater. Thus the perturbations of aerodynamic force and moment coefficients are set to be

$$\begin{cases} C'_L = (0.8 - 0.5\dfrac{\pi}{180}\alpha)C_L \\ C'_D = (1.2 + 0.5\dfrac{\pi}{180}\alpha)C_D \\ C'_m = (0.8 - 0.5\dfrac{\pi}{180}\alpha)C_m \end{cases} \tag{33}$$

where C' are the perturbation values, and C the rated values.

According to the aerodynamic parameter uncertainties in the model, the closed-loop response of the morphing aircraft during the wing folding process is shown in Fig. 8. It is seen that the parameter amplitude of the closed-loop response increases slightly due to the aerodynamic parameter perturbation. The motion of the morphing aircraft converges slower after wing folding is completed. Even so, the flight control system can still ensure that the speed variation in the wing morphing process is small, and that the altitude varies less than 1 m. This means the gain self-scheduled H_∞ robust control system can maintain good robustness under modeling uncertainty of aerodynamics.

5. Conclusion

(1) The LPV model for the folding-wing morphing aircraft in wing folding is derived from longitudinal nonlinear dynamic equations by using Jacobian linearization approach. The LPV model includes the variants of aerodynamic force and moment caused by wing folding, which can be regarded as a disturbance source. The dynamic response is simulated using the nonlinear model and LPV model. It is shown that the longitudinal LPV model obtained by Jacobian linearization approach can capture the morphing aircraft's complex behavior in the wing transition process.

(2) In order to ensure that the morphing aircraft flies at a given altitude and speed in the wing folding process, an inner-loop optimal quadratic output feedback and outer-loop gain scheduled H_∞ robust controller based on convex optimization algorithm is designed. The simulations show that the control objective of maintaining

speed and altitude change only slightly when the wing folding process can be achieved via the multi-loop control approach. The morphing aircraft can rapidly return to stable flight when the wing completes folding. In addition, the multi-loop flight control system's robustness is verified according to the aerodynamic parameter uncertainties in the wing morphing dynamic model.

Acknowledgements

This study was co-supported by China Postdoctoral Science Foundation (Nos. 20110490259, 2012T50038).

Appendix A

$$\begin{cases} A = \begin{bmatrix} a_{11} & a_{12} & a_{13} & a_{14} \\ a_{21} & a_{22} & a_{23} & a_{24} \\ a_{31} & a_{32} & a_{33} & a_{34} \\ a_{41} & a_{42} & a_{43} & a_{44} \end{bmatrix} \\ B = \begin{bmatrix} b_{11} & b_{12} \\ b_{21} & b_{22} \\ b_{31} & b_{32} \\ b_{41} & b_{42} \end{bmatrix} \\ W = \begin{bmatrix} w_{11} \\ w_{21} \\ w_{31} \\ w_{41} \end{bmatrix} \end{cases} \tag{A1}$$

$$\begin{cases} a_{11} = -\dfrac{I_y}{mI_y - S_z^2} \cdot \left[\dfrac{1}{2}\rho V_0 S C_{DV} + \rho u_0 S(C_{D0} + C_{D\alpha}\alpha_0)\right] - \dfrac{S_z}{mI_y - S_z^2} \cdot \left[\dfrac{1}{2}\rho V_0 c S C_{mV} + \rho u_0 S c (C_{m0} + \dfrac{C_{m\alpha}}{C_{L\alpha}} C_{L0} + C_{m\alpha}\alpha_0 + C_{m\delta_e}\delta_{e0})\right] \\ a_{12} = -\dfrac{I_y}{mI_y - S_z^2} \cdot \left[\dfrac{1}{2}\rho V_0 S C_{D\alpha} + \rho w_0 S(C_{D0} + C_{D\alpha}\alpha_0)\right] - \dfrac{S_z}{mI_y - S_z^2} \cdot \left[\dfrac{1}{2}\rho V_0 c S C_{m\alpha} + \rho w_0 S c (C_{m0} + \dfrac{C_{m\alpha}}{C_{L\alpha}} C_{L0} + C_{m\alpha}\alpha_0 + C_{m\delta_e}\delta_{e0})\right] \\ a_{13} = \dfrac{I_y}{mI_y - S_z^2}(-mw_0 - 2\dot{S}_z) - \dfrac{S_z}{mI_y - S_z^2}(-\dot{I}_y - S_z w_0 + \dfrac{1}{4}\rho V_0 c^2 S C_{mq}) \\ a_{14} = -\dfrac{I_y}{mI_y - S_z^2} mg\cos\theta_0 + \dfrac{S_z}{mI_y - S_z^2} g S_z \cos\theta_0 \end{cases} \tag{A2}$$

$$\begin{cases} a_{21} = -\dfrac{1}{m}\left[\dfrac{1}{2}\rho V_0 S C_{LV} + \rho u_0 S(C_{D0} + C_{D\alpha}\alpha_0)\right] \\ a_{22} = -\dfrac{1}{m}\left[\dfrac{1}{2}\rho V_0 S C_{L\alpha} + \rho w_0 S(C_{D0} + C_{D\alpha}\alpha_0)\right] \\ a_{23} = u_0 \\ a_{24} = -g\sin\theta_0 \end{cases} \tag{A3}$$

$$\begin{cases} a_{31} = \dfrac{S_z}{mI_y - S_z^2} \cdot \left[\dfrac{1}{2}\rho V_0 S C_{DV} + \rho u_0 S(C_{D0} + C_{D\alpha}\alpha_0)\right] + \dfrac{m}{mI_y - S_z^2} \cdot \left[\dfrac{1}{2}\rho V_0 c S C_{mV} + \rho u_0 S c (C_{m0} + \dfrac{C_{m\alpha}}{C_{L\alpha}} C_{L0} + C_{m\alpha}\alpha_0 + C_{m\delta_e}\delta_{e0})\right] \\ a_{32} = \dfrac{S_z}{mI_y - S_z^2} \cdot \left[\dfrac{1}{2}\rho V_0 S C_{D\alpha} + \rho w_0 S(C_{D0} + C_{D\alpha}\alpha_0)\right] + \dfrac{m}{mI_y - S_z^2} \cdot \left[\dfrac{1}{2}\rho V_0 c S C_{m\alpha} + \rho w_0 S c (C_{m0} + \dfrac{C_{m\alpha}}{C_{L\alpha}} C_{L0} + C_{m\alpha}\alpha_0 + C_{m\delta_e}\delta_{e0})\right] \\ a_{33} = -\dfrac{S_z}{mI_y - S_z^2}(-mw_0 - 2\dot{S}_z) + \dfrac{m}{mI_y - S_z^2}(-\dot{I}_y - S_z w_0 + \dfrac{1}{4}\rho V_0 c^2 S C_{mq}) \\ a_{34} = \dfrac{S_z}{mI_y - S_z^2} mg\cos\theta_0 - \dfrac{m}{mI_y - S_z^2} g S_z \cos\theta_0 \end{cases} \tag{A4}$$

$$a_{41} = 0, \quad a_{42} = 0, \quad a_{43} = 1, \quad a_{24} = 0 \tag{A5}$$

$$\begin{cases} b_{11} = -\dfrac{I_y}{mI_y - S_z^2}\dfrac{1}{2}\rho V_0^2 S C_{D\delta_e} - \dfrac{S_z}{mI_y - S_z^2}\dfrac{1}{2}\rho V_0^2 c S C_{m\delta_e} \\ b_{21} = -\dfrac{1}{m}\dfrac{1}{2}\rho V_0^2 S C_{L\delta_e} \\ b_{31} = \dfrac{S_z}{mI_y - S_z^2}\dfrac{1}{2}\rho V_0^2 S C_{D\delta_e} + \dfrac{m}{mI_y - S_z^2}\dfrac{1}{2}\rho V_0^2 c S C_{m\delta_e} \\ b_{41} = 0 \\ b_{12} = \dfrac{I_y}{mI_y - S_z^2} T_{\delta_p} \\ b_{22} = 0 \\ b_{32} = -\dfrac{S_z}{mI_y - S_z^2} T_{\delta_p} \\ b_{42} = 0 \end{cases} \tag{A6}$$

$$\begin{cases} w_{11} = \dfrac{I_y}{mI_y - S_z^2}\left[-\dfrac{1}{2}\rho V_0^2 S(C_{D0} + C_{D\alpha}\alpha_0) + T_0 - mg\sin\theta_0\right] - \dfrac{S_z}{mI_y - S_z^2}\left[2S_{1x}\ddot{S}_{1z}/m_1 + 2S_{2x}\ddot{S}_{2z}/m_2 + \dfrac{1}{2}\rho V_0^2 c S \cdot (C_{m0} + \dfrac{C_{m\alpha}}{C_{L\alpha}} C_{L0} + C_{m\alpha}\alpha_0 + C_{m\delta_e}\delta_{e0}) - g S_z \sin\theta_0\right] \\ w_{21} = \dfrac{1}{m}\left[-\dfrac{1}{2}\rho V_0^2 S(C_{L0} + C_{L\alpha}\alpha_0) + mg\cos\theta_0\right] \\ w_{31} = -\dfrac{S_z}{mI_y - S_z^2}\left[-\dfrac{1}{2}\rho V_0^2 S(C_{D0} + C_{D\alpha}\alpha_0) + T_0 - mg\sin\theta_0\right] + \dfrac{m}{mI_y - S_z^2}\left[2S_{1x}\ddot{S}_{1z}/m_1 + 2S_{2x}\ddot{S}_{2z}/m_2 + \dfrac{1}{2}\rho V_0^2 c S \cdot (C_{m0} + \dfrac{C_{m\alpha}}{C_{L\alpha}} C_{L0} + C_{m\alpha}\alpha_0 + C_{m\delta_e}\delta_{e0}) - g S_z \sin\theta_0\right] \\ w_{41} = 0 \end{cases} \tag{A7}$$

References

1. Wlezien RW, Horner GC, McGowan AR, Padula SL, Scott MA, Silcox RJ, et al. The aircraft morphing, program. AIAA-1998-1927; 1998.
2. Wilson JR. Morphing UAVs change the shape of warfare. *Aerosp Am* 2004;**42**(2):28–9.

3. Bowman JC, Plumley RW, Dubois JA, Wright DM. Mission effectiveness comparisons of morphing and non-morphing vehicles. AIAA-2006-7771; 2006.
4. Yue T, Wang LX, Ai JQ. Key technologies in morphing aircraft design. *Flight Dyn* 2009;**27**(5):6–10 [Chinese].
5. Seigler TM, Neal DA. Analysis of transition stability for morphing aircraft. *J Guidance Control Dyn* 2009;**32**(6):1947–53.
6. Obradovic B, Subbarao K. Modeling of flight dynamics of morphing-wing aircraft. *J Aircraft* 2011;**48**(2):391–401.
7. Obradovic B, Subbarao K. Modeling of dynamic loading of morphing-wing aircraft. *J Aircraft* 2011;**48**(2):424–35.
8. Seigler TM, Neal DA, Bae JS, Inman DJ. Modeling and flight control of large-scale morphing aircraft. *J Aircraft* 2007;**44**(4):1077–87.
9. Ataei-Esfahani A, Wang Q. Robust failure compensation for a morphing aircraft model using a probabilistic approach. *IEEE Trans Control Syst Technol* 2007;**15**(2):324–31.
10. Valasek J, Tandale MD, Rong J. A reinforcement learning-adaptive control architecture for morphing. AIAA-2004-6220; 2004.
11. Baldelli DH, Lee D, Sánchez Peña RS. Modeling and control of an aeroelastic morphing vehicle. *J Guidance Control Dyn* 2008;**31**(6):1687–99.
12. Spillman MS. Robust longitudinal flight control design using linear parameter varying feedback. *J Guidance Control Dyn* 2000;**23**(1):101–8.
13. Biannic J, Apkarian P, Garrard WL. Parameter varying control of a high-performance aircraft. *J Guidance Control Dyn* 1997;**20**(2):225–31.
14. Natesan K, Gu D, Postlethwaite I. Design of static H_∞ linear parameter varying controllers for unmanned aircraft. *J Guidance Control Dyn* 2007;**30**(6):1822–7.
15. Apkarian P, Gahinet P, Becker G. Self-scheduled H_∞ control of linear parameter varying systems: a design example. *Automatica* 1995;**31**(9):1251–61.
16. Yue T, Wang LX, Ai JQ. Longitudinal multibody dynamic characristics of Z-wing morphing aircraft. *Acta Aeronaut Astronaut Sin* 2010;**31**(4):679–86 [Chinese].
17. Marcos A, Balas G. Linear parameter varying modeling of the Boeing 747–100/200 longitudinal motion. AIAA-2001-4347; 2001.
18. Kumar A, Andersen MR. A comparision of LPV modelling techniques for aircraft, control. AIAA-2000-4458; 2000.
19. Marcos A, Balas GJ. Development of linear-parameter-varying models for aircraft. *J Guidance Control Dyn* 2004;**27**(2):218–28.
20. Shin JY, Balas GJ, Kaya MA. Blending methodology of linear parameter varying control synthesis of F-16 aircraft system. *J Guidance Control Dyn* 2002;**25**(6):1040–8.
21. Stevens BL, Lewis FL. *Aircraft control and simulation*. 2nd ed. New York: John Wiley & Sons, Inc.; 2003.
22. Nelder JA. A simplex method for function minimization. *Comput J* 1964;**7**(4):308–13.
23. Huang YG, McColl WF. An improved simplex method for function minimization. *Comput-Aided Des Arch* 2006;**4**(2):71–8.

Yue Ting is a postdoctor at School of Aeronautic Science and Engineering, Beihang University. He received the B.S., M.S. and Ph.D. degrees in aircraft design from Beihang University in 2004, 2006 and 2010 respectively. His main research interest is aircraft flight dynamics and control.

Wang Lixin is a professor in Beihang University. His main research interest lies in aircraft design, flight dynamics and flight control.

Ai Junqiang is a researcher in The First Aircraft Design Institute of AVIC. His main research interest lies in aircraft design.